LDA INVESTIGATION OF A TRANSONIC BUMP FLOW

H. Babinsky, S. Prioris

Cambridge University Engineering Department Trumpington Street, Cambridge, CB2 1PZ, UK

<u>Summary</u> The transonic flow over a circular arc bump has been investigated in a blow-down wind-tunnel. A variety of shock strengths between M=1 2 and M=1.48, depending on the experimental configuration, were studied. Laser Doppler Anemometry has been used to gather detailed information on turbulent flow properties. The results highlight the effects of favourable and adverse pressure gradients on turbulence properties, in particular the influence of shock waves and separation / reattachment.

BACKGROUND AND MOTIVATION

In many transonic and supersonic flows of practical importance the interaction of a shock wave with a boundary layer plays a critical role. Shock wave / boundary layer interactions (SWBLIs) not only significantly influence local features, but they can also strongly affect the global flow by causing separation or by changing boundary layer characteristics for a large distance downstream. In terms of simulation, the computation of SWBLI is arduous for two main reasons. The first one is the complex nature of the flow physics due to the high level of interdependence between the shock wave and the boundary layer. For instance, the disturbance/recovery process in the boundary layer is generally not predicted correctly when extensive separation occurs. The second difficulty is the high Reynolds numbers encountered when trying to simulate full-scale flows. Typically for in-flight conditions, the Reynolds number based on the displacement thickness varies between 10,000 and 30,000 whereas Direct Numerical Simulation (DNS) can currently only provide results for Reynolds numbers in the 1000s. One alternative solution is to use Reynolds Averaged Numerical Simulation (RANS) methods. However, the accuracy of such codes relies on the ability of the turbulence model to reproduce the fundamental mechanisms of turbulence production and dissipation through the interaction. This requires the model to be calibrated and tested against experimental data, which is not widely available.

In this experiment, the case of a normal shock interacting with a boundary layer developing over a circular arc bump (as shown schematically in Fig.1) is studied because it makes it possible to investigate a wide range of SWBLI configurations on the same geometry. By varying the back-pressure in the wind tunnel the location and strength of the shock wave can be adjusted to achieve a number of configurations ranging from a weak shock without separation to a strong shock with extensive separation. The experiment was designed to provide a detailed SWBLI database including turbulent properties measured using Laser Doppler Anemometry (LDA) for comparison with RANS and DNS calculations. Furthermore, it is intended to provide further insight into the fundamental physical mechanisms driving SWBLI at realistic Reynolds numbers.

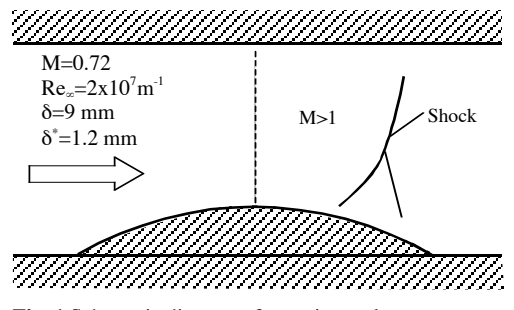


Fig. 1 Schematic diagram of experimental set-up

EXPERIMENTAL SET-UP

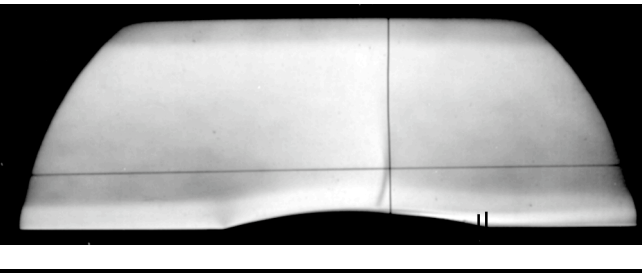
The experiments were performed in a transonic blow-down wind tunnel. Total conditions in the settling chamber ($T_t = 290 \text{ K}$, $P_t = 184 \text{ kPa}$) were maintained constant to within 2% while the pressure downstream of the test section (and therefore the flow configuration) was controlled using an adjustable second throat. A circular bump is fitted on the floor of the test section as shown in Fig. 1. The incoming boundary layer upstream of the bump is fully turbulent with a displacement thickness of 0.75 mm yielding a Reynolds number $Re_{\delta^*} = 24,000$.

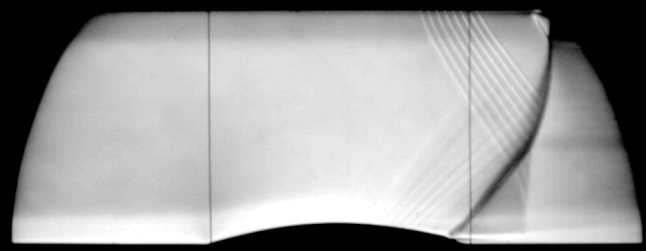
A two-dimensional LDA system was used to obtain measurements of normal and streamwise instantaneous velocity. The measuring volume is an ellipsoid of 75mm in diameter in the measuring plane and 1.88 mm in the transverse direction (effective integration width). The dynamic ranges of the LDA processors are respectively for each component [-160; +610] m/s and [-150; +580] m/s. The receiving optics were offset relatively to the axis of the emitting optics in order to prevent optical noise due to the light scattering from the test section floor or windows. A physical beam-stop was employed so that the maximum lens aperture could be used on the receiving optics to improve detection. This allowed measurements as close as 0.1 mm from the wall (y_{min}^+ <80-100) except around the trailing edge where optical access difficulties and a reduced signal-to-noise ratio was experienced. Boundary layer traverses typically explored twenty points - the number of measurement locations being limited by the running time of the wind tunnel. In order to allow for reliable statistical post-processing, at least 1000 coincident and validated velocity samples were recorded at each traverse location, although most data presented here were obtained with significantly higher numbers of samples (several 1000s). In the calculation of turbulent kinetic energy, the contribution of the unknown transverse velocity fluctuation <w'> was taken equal to an average contribution between both streamwise and normal velocity fluctuations. Although oil flow patterns revealed three-dimensional effects in the vicinity of the side-walls, the flow kept displaying a two-dimensional behaviour around the centreline for all cases. The measuring volume was always well within this region.

The flow was seeded using olive oil droplets with an average size of around 250 nm. This ensured a negligible level of lag in regions of high velocity gradients. In order to remove any velocity-induced bias on average quantities, the velocity measurements were weighted using the transit time, i.e. the residency time of each particle within the measuring volume. Indeed, arithmetic weighting is only appropriate if all velocity samples are independent; otherwise, it can introduce a bias towards higher velocities. In these experiments, transit times as short as 50 ns were recorded and used for all statistical analysis.

RESULTS AND DISCUSSION

In total four configurations were investigated in detail. These ranged from a very weak shock (below incipient separation) as seen in Fig.2 (top) to a strong shock located at the trailing edge of the bump as shown in Fig.2 (bottom). In both cases separation was present at the trailing edge, in the former case caused by the abrupt change of curvature at the trailing edge alone, and in the latter case due to the combined effects of geometry and the shock induced pressure gradient. The two configurations not shown here displayed flowfields in between these two extremes. Detailed LDA information has been obtained for all configurations allowing the presentation of u, v, u', v', turbulent shear stress and turbulent kinetic energy throughout the flowfield. As an example, Fig.3 shows the Reynolds shear stress <u'v'> for the configurations seen in Fig.2. Note that only the area starting at the crest of the bump is seen in these figures. The results clearly show the significant increase in Reynolds shear Fig.2 Schlieren photographs of configurations 1&4 stress near the shock wave and at separation. In





configuration 1 it is possible to distinguish between the effects of the shock and the separation occurring at the trailing edge. In configuration 4, the compactness of the separated region and the closeness of the shock wave and the trailing edge causes the effects of the shock, separation and re-attachment to all merge together.

The full paper will give more detail, concentrating in particular on:

- The flow development due to the presence of a strong favourable pressure gradient by comparing boundary layer properties upstream and on the crest of the bump.
- The flow properties in the interaction and separation regions
- The recovery of the boundary layer downstream of the bump after re-attachment.

By further analysis of the LDA data it has also been possible to obtain an estimate of the transverse pressure gradient in the boundary layer up to the interaction. This has revealed that the wall normal pressure gradients (often assumed to be negligible) are of the same order as the streamwise pressure gradients in most of the flow. This is caused by the considerable curvature of the flow and has implications for the numerical modelling of similar flows such as over aerofoils and turbine blades.

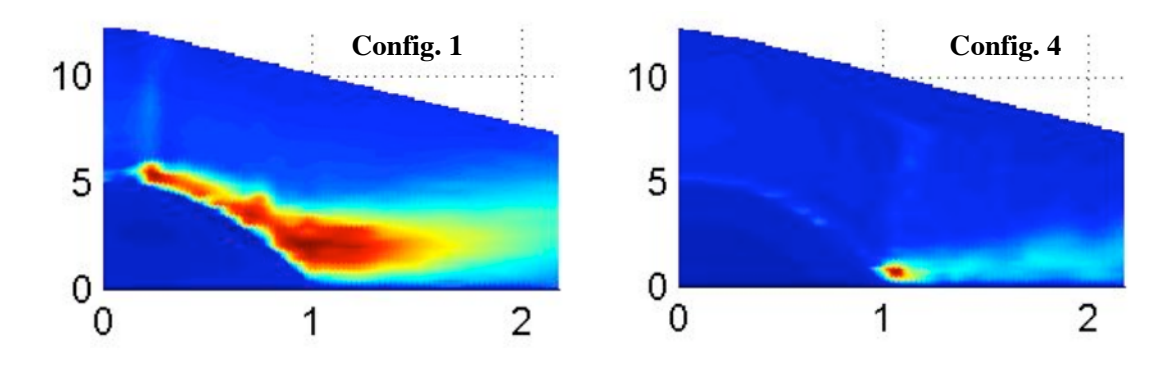


Fig.3 Map of Reynolds shear stress <u'v'> for configurations 1&4